

# Mechanical properties of brain tissue in-vivo: experiment and computer simulation

Karol Miller<sup>a,\*</sup>, Kiyoyuki Chinzei<sup>b</sup>, Girma Orssengo<sup>a</sup>, Piotr Bednarz<sup>c</sup>

<sup>a</sup>*Department of Mechanical and Materials Engineering, The University of Western Australia, Nedlands/Perth, WA 6907, Australia*

<sup>b</sup>*Biomechanics Division, Mechanical Engineering Laboratory, MITI, Namiki 1-2, Tsukuba, Ibaraki 305, Japan*

<sup>c</sup>*Polish Academy of Sciences, Institute of Fundamental Technological Research, ul. Swietokrzyska 21, Warsaw, Poland*

Accepted 22 May 2000

## Abstract

Realistic computer simulation of neurosurgical procedures requires incorporation of the mechanical properties of brain tissue in the mathematical model. Possible applications of computer simulation of neurosurgery include non-rigid registration, virtual reality training and operation planning systems and robotic devices to perform minimally invasive brain surgery. A number of constitutive models of brain tissue, both single-phase and bi-phasic, have been proposed in recent years. The major deficiency of most of them, however, is the fact that they were identified using experimental data obtained in vitro and there is no certainty whether they can be applied in the realistic in vivo setting. In this paper we attempt to show that previously proposed by us hyper-viscoelastic constitutive model of brain tissue can be applied to simulating surgical procedures. An in vivo indentation experiment is described. The force–displacement curve for the loading speed typical for surgical procedures is concave upward containing no linear portion from which a meaningful elastic modulus might be determined. In order to properly analyse experimental data, a three-dimensional, non-linear finite element model of the brain was developed. Magnetic resonance imaging techniques were used to obtain geometric information needed for the model. The shape of the force–displacement curve obtained using the numerical solution was very similar to the experimental one. The predicted forces were about 31% lower than those recorded during the experiment. Having in mind that the coefficients in the model had been identified based on experimental data obtained in vitro, and large variability of mechanical properties of biological tissues, such agreement can be considered as very good. By appropriately increasing material parameters describing instantaneous stiffness of the tissue one is able, without changing the structure of the model, to reproduce experimental curve almost perfectly. Numerical studies showed also that the linear, viscoelastic model of brain tissue is not appropriate for the modelling brain tissue deformation even for moderate strains. © 2000 Elsevier Science Ltd. All rights reserved.

**Keywords:** Brain tissue; Mechanical properties; Finite element simulation; Experiment in vivo

## 1. Introduction

More than 30 years of research into the mechanical properties of the brain and brain tissue was motivated by traumatic injury prevention (e.g. automotive accidents, see Chu et al., 1994; Ruan et al., 1994; DiMasi and Eppinger, 1995; Mendis et al., 1995; Kumaresan and Radhakrishnan, 1996; Voo et al., 1996; Arbogast and Margulies, 1997; Nishimoto and Murakami, 1998; Al-Bsharat et al., 1999) and understanding of brain structural deceases (e.g. hydrocephalus, see Nagashima et al., 1990; Kaczmarek et al., 1997).

In recent years, driven by developments in virtual reality techniques (Burdea, 1996) and the emergence of automatic surgical tools and robots (e.g. Brett et al., 1995), new exciting area of research has emerged — computer simulation of surgical procedures. The prerequisite for such a simulation is an appropriate mathematical model of the brain mechanical properties. This includes faithful representation of geometry, boundary and loading conditions as well as material properties of the brain.

Computer programs enabling accurate modelling of soft tissue deformation may find applications, for example, in a surgical robot control system, where the prediction of deformation is needed (Miller and Chinzei, 1995a, b), surgical operation planning and surgeon training systems based on the virtual reality techniques (Burdea, 1996 and references cited therein), where force

\* Corresponding author. Fax: + 61-8-9380-1024.

E-mail address: kmiller@mech.uwa.edu.au (K. Miller).

feedback is needed, and registration (Lavallée, 1995), where knowledge of local deformation is required.

The distinguishing feature of the mathematical model of the brain intended for the simulation of neurosurgery is the strain rate range (the loading speed range) considered —  $0.01\text{--}1.0\text{ s}^{-1}$  — orders of magnitude lower than that experienced in situations leading to injury. During loading resulting in such strain rates both non-linear stress — strain and stress — strain rate relations demonstrate their importance (Miller and Chinzei, 1997).

There is a wealth of information available in the literature about the mechanical properties of brain tissue in vitro (Ommaya, 1968; Estes and McElhaney, 1970; Galford and McElhaney, 1970; Pamidi and Advani, 1978; Bilston et al., 1997; Donnelly and Medige, 1997; Miller and Chinzei, 1997). The question, whether the mathematical models of the brain tissue mechanical properties based on these data can be applied to more realistic in vivo conditions was investigated in Metz et al. (1970). However, Metz and co-workers gave no indication of loading speeds applied, which severely limits the utility of that paper. Other researchers attempting to characterise brain tissue properties in vivo include Walsh and Schettini (1984), and Sahay et al. (1992).

In this paper we intend to prove that the hyper-viscoelastic model based on the strain energy function in polynomial form with time-dependent coefficients (Miller, 1999), is suitable for description of brain tissue deformation behaviour in vivo, at low strain rates, typical for surgical procedures, and that the slight adjustment of material parameters describing the instantaneous stiffness of the tissue, without altering the structure of the model, results in almost perfect reproduction of the experimental curve obtained in vivo.

## 2. Indentation of swine brain tissue in vivo

### 2.1. Experimental set-up

We conducted an indentation experiment on the exposed brain of an approximately 100-day-old Landrace swine under anaesthesia. The weight of the swine was approximately 50 kg. The experiment was performed in the Surgeon Training Facility in Fujinomiya, Japan.

The brain was exposed by removing the skin, the skull and the dura. The exposed region, located on the front lobe, was of oval shape, approximately  $25 \times 20$  mm. After exposing the brain, the head was fixated into a metallic frame with four sharp-end screws.

The main testing apparatus was a two-linear-degree-of-freedom robot equipped with a strain-gauge load cell. The robot, fixed onto a rigid support, drove a cylindrical indenter of 10 mm diameter. This allowed the flexibility of choosing the loading velocity and the depth of the indentation. Fig. 1 shows the experimental setting.

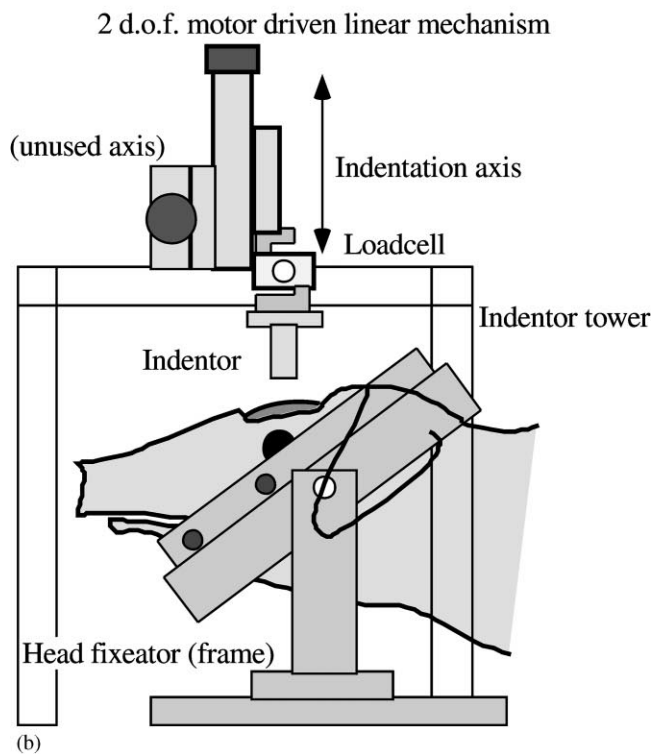


Fig. 1. In vivo indentation of swine brain-experiment configuration: (a) general view; and (b) schematic of the set-up.

### 2.2. Data acquisition and processing

Based on the estimates of the speed of surgeon's hands when conducting brain tissue separation (observed by the authors in Tokyo Women's Medical College Hospital), an indenter velocity of  $1\text{ mm s}^{-1}$  was applied. The maximum depth of penetration of 3.9 mm was set. The choice of the depth was based on our vast experience with swine brain tissue. We expected that the deeper indentation might inadvertently damage the brain and consequently kill the animal. The applied force was measured by a

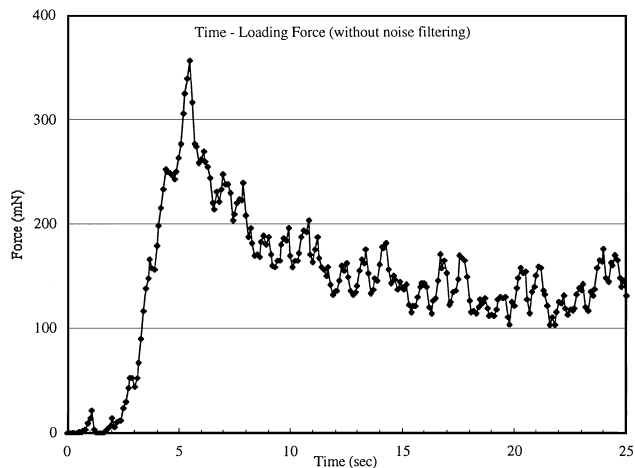


Fig. 2. Measured force versus time force curve for the indentation of brain tissue. The influence of the heartbeat and the respiration is apparent.

sensitive load cell manufactured in the Mechanical Engineering Laboratory, Japan (max. load 0.98 N, max. displacement 0.1 mm, linearity 0.035%, hysteresis 0.040%). The signal from the load cell was acquired by a PC using a 12-bits analog-to-digital converter.

Fig. 2 shows a measured force versus time curve. The influence of the heartbeat and the respiration is very apparent, however the removal of the corresponding frequencies did not pose any difficulty. The filtered result, together with theoretical predictions, is shown in Fig. 7.

### 2.3. Imaging technique and image analysis

At the end of the experiment, the swine was sacrificed by a KCl injection. Then, in order to obtain the precise information on the geometry of the brain, magnetic resonance (MR) images of the head were acquired. The imaging was performed in the Department of Precision Engineering of Tokyo University. The sequence used was the 3D Gradient Field Echo, repetition/echo time (TR/TE) = 250/20 ms (T1 weighted scan), field of view (FOV) =  $160 \times 160 \times 64$  mm, resolution =  $128 \times 128 \times 32$  pixels, flip angle =  $90^\circ$ , number of data ac-

quisition (NEX) = 1. The scanner was Hitachi MRH500, 0.5 T superconducting magnet. Fig. 3 shows examples of the axial slices of the obtained image. The images were taken approx. 3 h after the swine was sacrificed. This delay might have introduced some changes to the brain geometry, e.g. due to swelling. We assumed in our work that the changes were small and did not affect conclusions of our paper.

## 3. Finite element modelling of compression of swine brain in vivo

### 3.1. Finite element mesh

To analyse the experimental results and consequently prove the appropriateness of the constitutive model proposed in Miller (1999) a comprehensive, three-dimensional, non-linear, finite element model of the experiment was developed.

The mesh was constructed, using PATRAN (1998), from the magnetic resonance images of the coronal sections of the brain (Fig. 3). A schematic diagram of the coronal section of a swine brain is shown in Fig. 4. To facilitate the construction of the mesh, the section boundary was divided into four curves AB, BC, CD, and DA, determined by fitting smooth curves through six points obtained from the resonance image. Using these four curves, and the vertical and horizontal lines shown in Fig. 4, four surfaces were defined to represent the coronal section. Similarly, four surfaces were created for all of the other coronal section images. The distance between successive sections was 5 mm. Sixteen sections were used to construct the mesh. The corresponding surfaces in successive sections were used to define solids. Eight-noded hexagonal finite elements (element type C3D8H in ABAQUS, ABAQUS, 1998) were created on all the solids. The finite element meshes are shown in Fig. 5. As the model was developed from the sectional images, the front surface obtained from the first sectional image has a flat surface. The front surface is well away from the area of application of the load so that its exact shape does not affect the result for the force–displacement relationship.

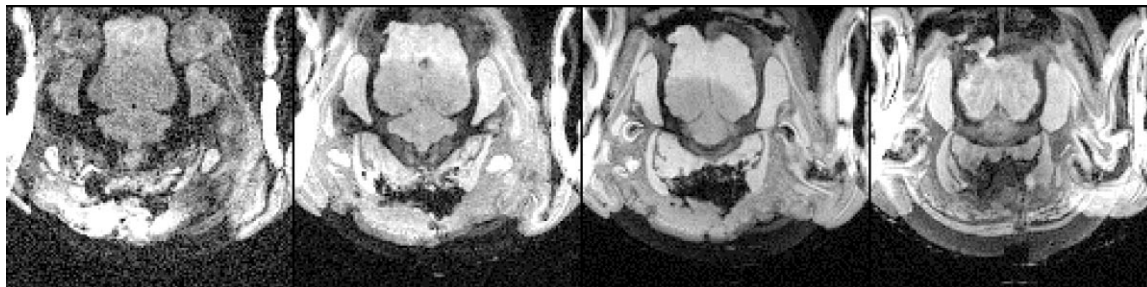


Fig. 3. T1 weighted MR scans of the swine head.

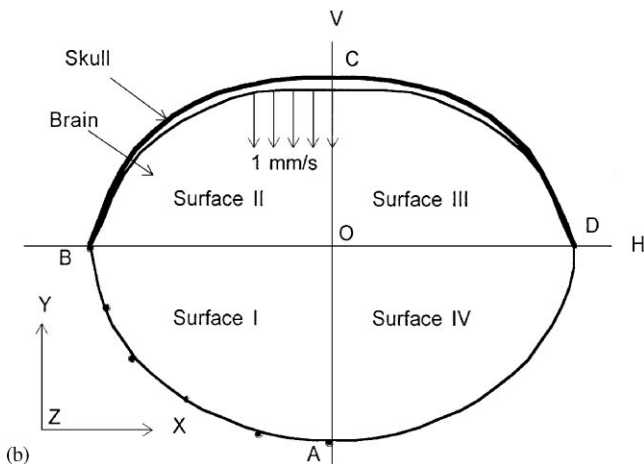
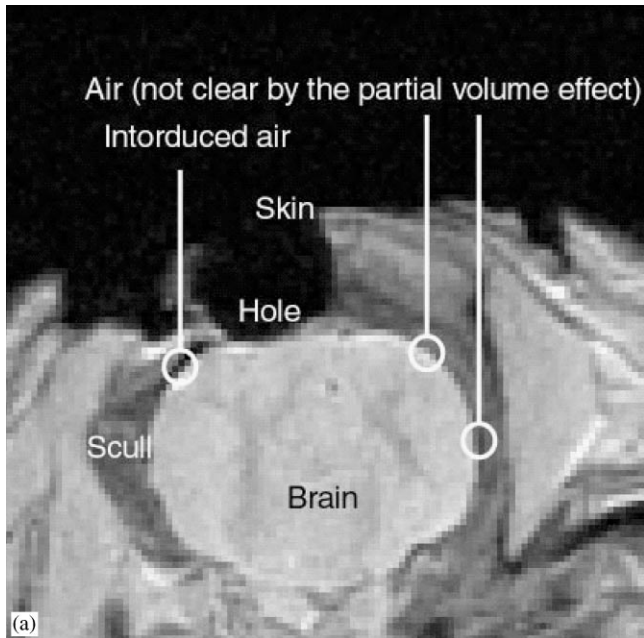


Fig. 4. (a) MR sectional image; and (b) construction of the three-dimensional finite element mesh of the swine brain from its coronal section images.

### 3.2. Constitutive model of brain tissue

In the finite element modelling, the material properties of the brain tissue used were taken from the experimental, analytical, and finite element results of Miller (1999). The model was identified based on in vitro unconfined compression tests.

The hyper-viscoelastic constitutive model developed in Miller (1999) is based on the strain energy function in the form of a convolution integral:

$$W = \int_0^t \left\{ \sum_{i+j=1}^N \left[ C_{ij0} \left( 1 - \sum_{k=1}^n g_k (1 - e^{-t-\tau/\tau_k}) \right) \right] \right. \\ \left. \times \frac{d}{d\tau} [(J_1 - 3)^i (J_2 - 3)^j] \right\} d\tau, \quad (1)$$

where  $\tau_k$  are characteristic times,  $g_k$  are relaxation coefficients,  $N$  is the order of polynomial in strain invariants (as a result of the assumption of the brain tissue initial isotropy the energy depends on the histories of strain invariants only) used for strain energy function description, and  $J_1, J_2, J_3$  are strain invariants. The common assumption of brain tissue incompressibility results in the third invariant being equal to 1.

The material constants, obtained by rather complicated, iterative procedure (Miller, 1999) are listed in Table 1. The proposed model is linear in material coefficients  $C_{ij0}$  (Miller, 1999).

It is important to note that we used average (six brains were used) mechanical properties identified in vitro to simulate deformation of the brain of the specific swine in vivo, so that, the exact agreement of numerical calculations with the experiment was not expected.

### 3.3. Boundary conditions

In the in vivo experiment, the brain tissue was compressed at a velocity of  $1 \text{ mm s}^{-1}$  using the end effector of 10 mm diameter. To model this loading, the nodes on the top surface of the finite element model were moved to form a circular area of 10 mm diameter as shown in Fig. 5. During compression of the brain, all the nodes within this circular area have the same velocity. This condition was implemented in MSC/PATRAN (PATRAN, 1998).

We assumed that the bottom surface of the brain, denoted by curve DAB in Fig. 4, does not move. Therefore, all nodes on this surface were fixed. However, the top surface of the brain, denoted by BCD in Fig. 4, moves when the applied velocity is applied, so this surface was left free to deform.

### 3.4. Mesh convergence study

To determine whether the meshes shown in Fig. 5 were satisfactory, the results obtained with each of them were compared. The difference in results obtained with the dense and intermediate mesh, which has three times fewer nodes, is less than 1%. The force calculated with a coarse mesh is about 5% higher than that estimated with finer meshes. This gives evidence that the finite element approximation has converged and the results are satisfactory. In the subsequent analysis, the model shown in Fig. 5c was chosen, because to obtain results from this model takes 10% of the analysis time required to obtain results from the model shown in Fig. 5b, while the results from the two models are practically identical.

### 3.5. Modelling the skull

In the vicinity of the indenter the brain tissue moves away from the skull. In contrast, in order to satisfy the

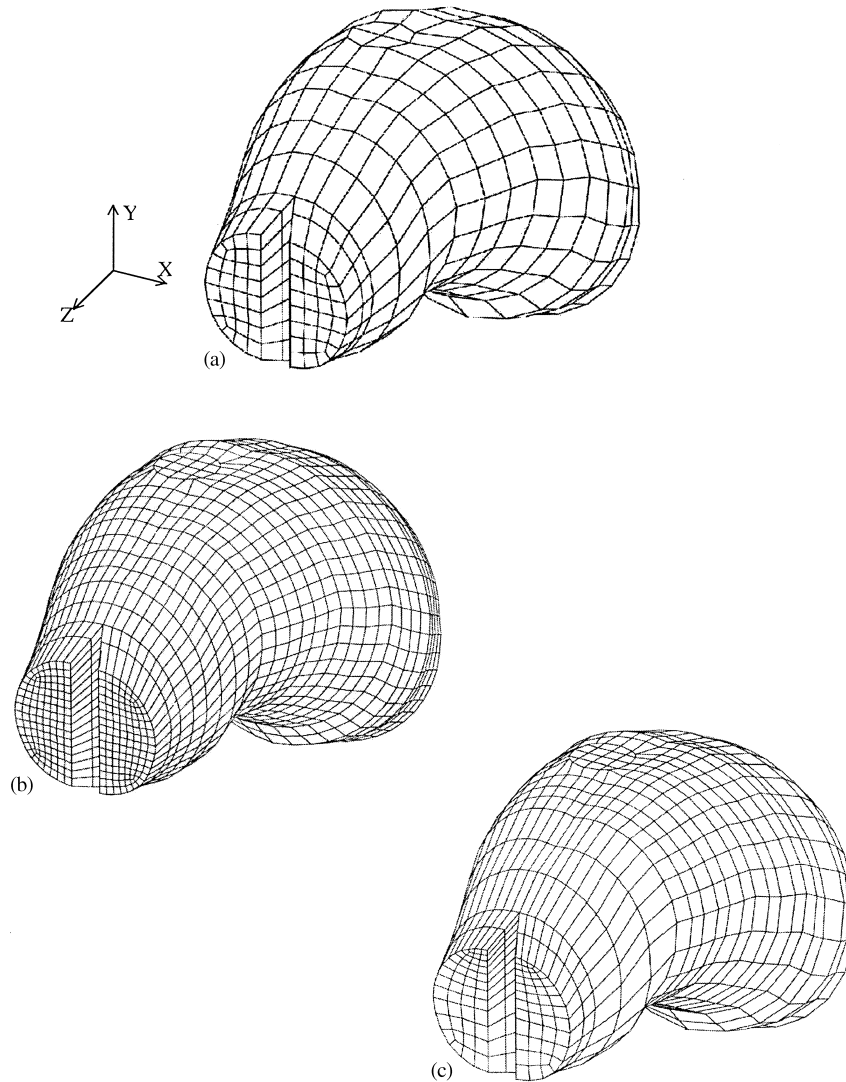


Fig. 5. Finite element meshes of the swine brain constructed from its coronal section images: (a) coarse mesh, 1259 nodes and 960 eight-noded hexagonal elements; (b) dense mesh, 8249 nodes and 7200 hexagonal elements; and (c) intermediate mesh with high density in the vicinity of the indenter, 2533 nodes and 2024 hexagonal elements. The length of the model along the  $z$ -axis is 75 mm and its maximum width along the  $x$ -axis is 50 mm.

Table 1  
Material properties of swine brain tissue (Miller, 1999)

Instantaneous response	Characteristic time $t_1 = 0.5$ (s)	Characteristic time $t_2 = 50$ (s)
$C_{100} = C_{010} = 263$ (Pa)	$g_1 = 0.450$	$g_2 = 0.365$
$C_{200} = C_{020} = 491$ (Pa)		
$C_{110} = 0$		

condition of the incompressibility (assumed in the constitutive model of the brain tissue), the top portion of the brain farther from the indenter should move towards the skull. Obviously, the tissue cannot move outside the volume limited by the skull. To obtain a realistic finite element model for the indentation of brain tissue *in vivo*,

this condition had to be appropriately modelled. A frictionless sliding contact between the brain tissue and the skull was chosen for a boundary condition for the upper-half of the brain surface.

This also required an appropriate choice of the size of the gap between the brain surface and the skull. Due to the weight of the brain and the tissue's ability to move horizontally, the gap between the skull and the brain was assumed to vary as shown in Fig. 4, with the maximum gap at the top. The size of the gap should correspond to the thickness of the subarchnoid space. Unfortunately, to the best of our knowledge, the literature published to date does not contain these data. Therefore, we had to rely on our estimates based on magnetic resonance images taken. In the finest of our images the pixel size was 0.94 mm. The analysis of pixel values in the area of the

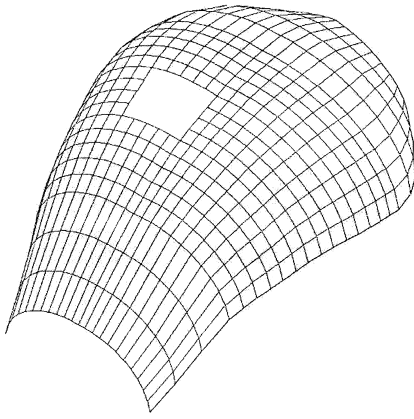


Fig. 6. Finite element mesh of the skull.

gap, taking into account the partial volume effect, led us to believe that the maximum gap width was slightly smaller than the pixel size. Therefore, in subsequent analyses, the maximum size of the gap was taken to be 0.75 mm.

In modelling the sliding contact between the brain and the skull, all the nodes of the skull surface were fixed. If contact is established between a node on the top surface of the brain model and an element edge of the skull model convergence problems may result. To avoid this, the nodes on the skull model were staggered relative to the nodes on the top surface of the brain model so that the brain nodes move toward the skull elements' centres, but not toward their edges. The finite element model of the skull surface is shown in Fig. 6.

#### 4. Results

Fig. 7 shows the comparison of the experimental force — displacement curve with computer simulation results using a hyper-viscoelastic, and linear viscoelastic constitutive models of brain tissue. Commercially available finite element software package ABAQUS (ABAQUS, 1998) was used. Non-linear geometrically (finite deformation) procedures were applied. The deformed shape of the brain is shown in Fig. 8.

The force predicted by the finite element model based on the hyper-viscoelastic constitutive equation for the brain tissue, at the indentation depth of 3.9 mm, is about 31% lower than that measured in vivo. Additionally, it is clear that even for moderate strains considered in this study, the linear-viscoelastic constitutive model is not appropriate and more advanced modelling techniques are required.

#### 5. Discussion and conclusions

This paper attempts at proving that the previously proposed constitutive model of brain tissue (Miller, 1999)

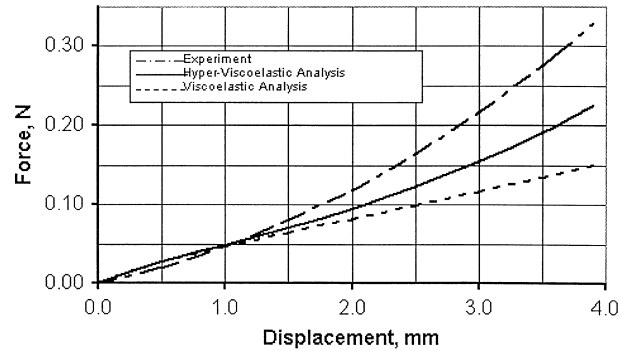


Fig. 7. Force versus displacement relationship for  $1 \text{ mm s}^{-1}$  indentation speed and 10 mm indenter diameter: (a) experiment; (b) hyper-viscoelastic analysis results; (c) linear, viscoelastic analysis results (for small strains the linear, viscoelastic model used had the same properties as the non-linear, hyper-viscoelastic model (Miller and Chinzei, 1997), instantaneous Young modulus  $E = 3240 \text{ Pa}$ , Poisson's ratio  $\nu = 0.499$ ).

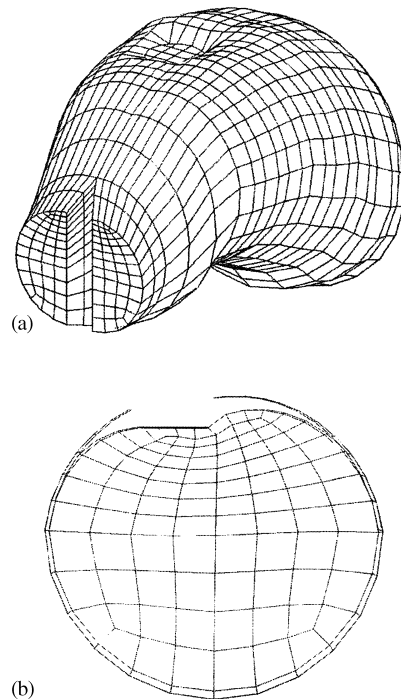


Fig. 8. Deformed brain mesh: (a) general view; and (b) sectional view.

can be applied in finite element simulation of brain deformation in vivo for moderate strain rates, and consequently, to neurosurgical simulation. The constitutive model used in this study was identified based on the series of in vitro tests.

The in vivo indentation experiment is described and its results analysed using a sophisticated, highly non-linear, three-dimensional finite element model. The forces predicted by this model are about 31% lower than the measured ones. Taking into account the large variability inherent to biological materials, and the apparent stiffening of the tissue due to the tethering effect of a large

number of blood vessels in the brain, the agreement, in our opinion, is good. The constitutive model used in this study is linear in parameters describing instantaneous response of the material (Miller, 1999). Therefore the increase of these parameters by 31% will result in almost perfect reproduction of the experimental force — displacement curve.

The apparent limitation of this study is that the *in vivo* experiment was conducted on one swine only. The proposed numerical model of the brain *in vivo* is intended to lead to computer simulation of neurosurgical procedures. Two cases have to be considered:

- (i) Surgical training system with realistic force feedback — such a system requires a model of an “average” brain, with most “common” mechanical properties. To delineate mechanical constants for such a system would require tests on humans to be conducted. The sacrifice of more pigs will not help.
- (ii) Surgical operation planning for a particular patient — in this case the model with “average” properties is not needed. We need to identify the properties of the patient. Our paper shows that the proposed methods can provide mathematical framework for modelling. The numerical values for parameters have to be ascertained for each patient considered.

At this point the methodology of conducting neurosurgical simulation can be suggested. Magnetic resonance images of a patient’s head can be used to construct the mesh. Delicate indentation of the brain can then serve as a tool to adjust material constants in the mathematical model, without altering the model structure. The resulting model can next be used with some degree of confidence. However, more research is needed, especially into the appropriate modelling of the interface between the brain and the skull (boundary conditions). This direction of research, in the authors’ opinion, is at least equally important to the investigation of the mechanical properties of brain internal structures.

Recently, Paulsen et al. (1999) conducted finite element simulation of the brain deformation based on the bi-phasic constitutive model of brain tissue. However, the finite element model used is linear, so that cannot be realistically applied to modelling surgical procedures, which invariably result in large displacements of the tissue. Moreover, as was shown in Miller (1998), the standard bi-phasic theory is unable to account for strong stress–strain rate dependence, which is an important characteristics of brain tissue mechanical properties. The hyper-viscoelastic modelling approach proposed here does not have such deficiencies.

### Acknowledgements

The financial support of Japanese Science and Technology Agency, Japanese Special Bilateral Cooperation

Funds and the Australian Research Council is gratefully acknowledged.

### References

- ABAQUS Theory Manual, 1998. Version 5.2. Hibbit, Karlsson & Sorensen, Inc., USA.
- Al-Bsharat, A., Zhou, C., Yang, K.H., Khalil, T., King, A.I., 1999. Intracranial pressure in the human head due to frontal impact based on a finite element model. Proceedings of ASME Summer Bioengineering Meeting, Montana, USA, pp. 159–160.
- Arbogast, K.B., Margulies, S.S., 1997. Regional differences in mechanical properties of the porcine central nervous system. Proceedings of the 41st Stapp Car Crash Conference, SAE, pp. 293–300.
- Bilston, L.E., Zizhen, L., Phan-Tien Nhah, 1997. Linear viscoelastic properties of bovine brain tissue in shear. *Biorheology* 34 (6) 377–385.
- Brett, P.N., Fraser, C.A., Henningan, M., Griffiths, M.V., Kamel, Y., 1995. Automatic surgical tools for penetrating flexible tissues. *IEEE Engineering and Medical Biology* 264–270.
- Burdea, G., 1996. Force and Touch Feedback for Virtual Reality. Wiley, New York.
- Chu, C.S., Lin, M.S., Huang, H.M., Lee, M.C., 1994. Finite element analysis of cerebral contusion. *Journal of Biomechanics* 27 (2), 187–194.
- DiMasi, F., Eppinger, R., 1995. Computational analysis of head impact response under car crash loadings. Proceedings of the 38th Stapp Car Crash Conference. SAE, Orlando, FL.
- Donnelly, B.R., Medige, L., 1997. Shear properties of human brain tissue. *Transactions of ASME. Journal of Biomechanical Engineering* 119 (4), 423–432.
- Estes, M.S., McElhaney, J.H., 1970. Response of brain tissue of compressive loading. ASME Paper No. 70-BHF-13.
- Galford, J.E., McElhaney, J.H., 1970. A viscoelastic study of scalp, brain and dura. *Journal of Biomechanics* 3, 211–221.
- Kaczmarek, M., Subramaniam, R.P., Neff, S.R., 1997. The hydro-mechanics of hydrocephalus: steady-state solutions for cylindrical geometry. *Bulletin of Mathematical Biology* 59 (2), 295–323.
- Kumaresan, S., Radhakrishnan, S., 1996. Importance of partitioning membranes of the brain and the influence of the neck in head injury modelling. *Medical Biology in Engineering and Computers* 34 (1), 27–32.
- Lavallée, S., 1995. Registration for Computer Integrated Surgery: Methodology, State of the Art. *Computer-Integrated Surgery*. MIT Press, Cambridge, MA, pp. 77–97.
- Mendis, K.K., Stalnaker, R.L., Advani, S.H., 1995. A constitutive relationship for large deformation finite element modeling of brain tissue. *Transactions of ASME. Journal of Biomechanical Engineering* 117, 279–285.
- Metz, H., McElhaney, J., Ommaya, A.K., 1970. A comparison of the elasticity of live, dead, and fixed brain tissue. *Journal of Biomechanics* 3, 453–458.
- Miller, K., 1999. Constitutive model of brain tissue suitable for finite element analysis of surgical procedures. *Journal of Biomechanics* 32, 531–537.
- Miller, K., 1998. Modelling soft tissue using biphasic theory — a word of caution. *Computational Methods in Biomechanical and Biomedical Engineering* 1, 261–263.
- Miller, K., Chinzei, K., 1995a. Modeling of soft tissues. *Mechanical Engineering Laboratory News* 12, 5–7 (in Japanese).
- Miller, K., Chinzei, K., 1995b. Modeling of soft tissues deformation. Proceedings of the Second International Symposium on Computer Aided Surgery, Tokyo Women’s Medical College, Shinjuku, Tokyo. *Journal of Computer Aided Surgery* 1 (Suppl.), 62–63.

- Miller, K., Chinzei, K., 1997. Constitutive modelling of brain tissue; experiment and theory. *Journal of Biomechanics* 30 (11/12), 1112–1115.
- Nagashima, T., Skirakuni, T., Rapoport, S.T., 1990. A two-dimensional, finite element analysis of vasogenic edema. *Neurologica Medica Chirugica* 30, 1–9.
- Nishimoto, T., Murakami, S., 1998. Relation between diffuse axonal injury and internal head structures on blunt impact. *Journal of Biomechanical Engineering* 120 (1), 140–147.
- Ommaya, A.K., 1968. Mechanical properties of tissues of the nervous system. *Journal of Biomechanics* 1, 127–138.
- Pamidi, M.R., Advani, S.H., 1978. Nonlinear constitutive relations for human brain tissue. *Transactions of ASME. Journal of Biomechanical Engineering* 100, 44–48.
- PATRAN, 1998. MSC Patran VERSION 7.5 Manual. PDA Engineering, California, USA.
- Paulsen, K.D., Miga, M.I., Kennedy, F.E., Hoops, P.J., Hartov, A., Roberts, D.W., 1999. A computational model for tracking subsurface tissue deformation during stereotactic neurosurgery. *IEEE Transactions on Biomedical Engineering* 46 (2), 213–225.
- Ruan, J.S., Khalil, T., King, A.I., 1994. Dynamic response of the human head to impact by three-dimensional finite element analysis. *Transactions of ASME, Journal of Biomechanical Engineering* 116, 44–50.
- Sahay, K.B., Mehrotra, R., Sachdeva, U., Banerji, A.K., 1992. Elastomechanical characterization of brain tissues. *Journal of Biomechanics* 25, 319–326.
- Voo, L., Kumaresan, S., Pintar, F.A., Yoganandan, N., Sances Jr., A., 1996. Finite-element models of the human head. *Medical Biology in Engineering and Computers*. 34, 375–381.
- Walsh, E.K., Schettini, A., 1984. Calculation of brain elastic parameters in vivo. *American Journal of Physiology* 247, R637–R700.